

.....

**MRI BRAIN TUMOUR DETECTION BY HISTOGRAM AND
SEGMENTATION BY MODIFIED GVF MODEL**

Selvaraj.D¹, Dhanasekaran.R²

¹Research Scholar, Department of Electronics and Communication Engineering
Sathyabama University, Chennai, India

²Director, Research, Syed Ammal Engineering College, Ramanathapuram, India
Email: ¹mails2selvaraj@yahoo.com, ²rdhanashekar@yahoo.com

ABSTRACT

A new method of image segmentation is proposed in this paper which combines histogram thresholding, modified gradient vector field and morphological operators. The non-brain regions are removed using mathematical morphological operators. Histogram thresholding is used to detect whether the brain is normal or abnormal i.e., it is used to detect the suspicious region or tumor. If the brain is abnormal then the modified GVF is used to detect the contour of the tumor. Else, if the brain is normal then no need to proceed to the segmentation step. Therefore, the time consumed for segmentation can be minimized. The proposed method is computationally efficient. It is successfully applied to many MRI brain images to detect the tumor and its geometrical dimension. Finally the performance measures are validated with those of human expert segmentation.

Key words: Skull stripping, Brain segmentation, Tumour segmentation, MRI brain image, Morphological operator, Feature extraction

I. INTRODUCTION

Medical imaging refers to the techniques and processes used to create images of the human body to reveal, diagnose or examine disease [3]. Medical imaging is considered to be the most significant advancement of all the contemporary medical technologies. The modern imaging technologies are Computed Tomography, Positron emission tomography (PET), Ultrasound, Magnetic resonance imaging (MRI) and more. Magnetic resonance imaging (MRI) is a popular means for noninvasive imaging of the human body. While MRI does not use harmful X-rays, an MRI “image” shows more detail than images generated by X-ray, computerized tomography (CT) [4]. MRI provides images with the exceptional contrast between various organs and tumors that is essential for medical diagnosis and therapy. The

advantages of magnetic resonance imaging (MRI) over other imaging modalities are its high spatial resolution and excellent discrimination of soft tissues. On the other hand, MRI provides a noninvasive method to get angiography and functional images and till now no side effect of MRI has been reported.

Magnetic resonance imaging (MRI) is an advanced medical imaging technique providing rich information about the human soft tissue anatomy. MRI technique has been widely used in the study of neural disorders. Tissue classification and segmentation are the key steps toward quantifying the shape and volume of different types of tissues, which are used for three-dimensional display and feature analysis to facilitate diagnosis and therapy. A typical MRI of a patient includes multi-modal information in three dimensions. Generally, each slice has three different types of image (T1-weighted, T2-weighted and Proton Density-weighted), which have different contrast affected by selection of pulse sequence parameters [5]. Brain is one of the most complex organs of a human body so it is a vexing problem to discriminate its various components and analyze its constituents. Common image processing and analysis techniques provide ineffective and futile outcomes. Magnetic resonance images are very common for brain image analysis. Magnetic Resonance Images (MRI) of the brain are invaluable tools to help physicians diagnose and treat various brain diseases including stroke, cancer, and epilepsy. The MRI of the normal brain can be divided into three regions other than the background, white matter (WM), gray matter (GM), and cerebrospinal fluid (CSF) or vasculature [6].

A great number of segmentation methods are available in the literature to segment images according to various criteria such as for example gray level, color, or texture. Image segmentation was, is and will be a major research topic for many image-processing researchers. Segmentation of brain MRI's is an important image processing procedure for both the physician and the brain researcher. The brain MRI offers a valuable method to perform pre-and-post surgical evaluations, which are keys to define procedures and to verify their effects. Therefore, it is necessary to develop algorithms to obtain robust image segmentation.

The rest of this paper is organized as follows: A brief review of researches relevant to the MRI brain tumor detection and segmentation technique is presented in section 2. In section 3, the overview of the proposed method is discussed. Section 4 gives the concept of brain tumor detection using bimodal histogram technique and also gives the concept of MGVF. The detailed experimental results and discussions are given in section 5. The conclusions are summed up in section 6.

II. RELATED WORKS

A plentiful of researches has been proposed by researchers for the MRI brain image segmentation and tumor detection techniques. A brief review of some of the recent researches is presented here.

Kharrat, A. *et al.* [7] have developed a methodology, where the brain tumor has been detected from the cerebral MRI images. The methodology includes three stages: enhancement, segmentation and classification. An enhancement process has been performed to enhance the quality of images as well as to reduce the risk of distinct regions fusion in the segmentation stage. Also, a mathematical morphology has been used to increase the contrast in MRI images. Then, the MRI images have been decomposed by applying a Wavelet Transform in the segmentation process. Finally, the suspicious regions or tumors have been

extracted by using a k-means algorithm. The feasibility and the performance of the proposed technique have been revealed from their experimental results on brain images.

Belma Dogdas *et al.* [8] have presented a technique for segmentation of skull and scalp in T1-weighted magnetic resonance images (MRIs) of the human head. The method uses mathematical morphological operations to generate realistic models of the skull, scalp, and brain that are suitable for electroencephalography (EEG) and magnetoencephalography (MEG) source modeling. They segment the brain using the Brain Surface Extractor algorithm; using this, they can ensure that the brain does not intersect the skull segmentation. They generated a scalp mask using a combination of thresholding and mathematical morphology. Finally, they mask the results with the scalp and brain volumes to ensure closed and nonintersecting skull boundaries.

Inan Gule *et al.* [9] have presented an image segmentation system to automatically segment and label brain MR images to show normal and abnormal brain tissues using self-organizing maps (SOM) and knowledge-based expert systems. The feature vector is used as an input to the SOM. SOM is used to over segment images and a knowledge-based expert system is used to join and label the segments.

John Chiveron *et al.* [10] have described an automatic statistical morphology skull stripper (SMSS) that uniquely exploits a statistical self-similarity measure and a 2-D brain mask to delineate the brain. The result of applying SMSS to 20 MRI data set volumes, including scans of both adult and infant subjects was also described. Quantitative performance assessment was undertaken with the use of brain masks provided by a brain segmentation expert. The performance was compared with an alternative technique known as brain extraction tool. The results suggested that SMSS is capable of skull-stripping neurological data with small amounts of over- and under-segmentation.

Wen-Feng Kuo *et al.* [11] have proposed a robust medical image segmentation technique, which combines watershed segmentation and the competitive Hopfield clustering network (CHCN) algorithm to minimize undesirable over-segmentation. A region merging method is presented, which is based on employing the region adjacency graph (RAG) to improve the quality of watershed segmentation. The performance of the proposed technique is evaluated through quantitative and qualitative validation experiments on benchmark images.

A new unsupervised MRI segmentation method based on self-organizing feature map was presented by Yan Li and Zheru Chi [13]. Their algorithm included extra spatial information about a pixel region by using a Markov Random Field (MRF) model. The MRF term improved the segmentation results without extra data samples in the training set. The cooperation of MRF into SOFM has shown its great potentials as MRF term models the smoothness of the segmented regions. It verified that the neighboring pixels should have similar segmentation assignment unless they are on the boundary of two distinct regions.

R. Mishra [12] has developed an efficient system, where the Brain Tumor has been diagnosed with higher accuracy using artificial neural network. After the extraction of features from MRI data by means of the wavelet packets, an artificial neural network has been employed to find out the normal and abnormal spectra. Normally, the benefit of wavelet packets is that it gives richest analysis when compared with the wavelet transforms and thus adding more advantages to the performance of their proposed system. Moreover, two cancer detection approaches have been discussed. The neural network system has been trained using the Error Back Propagation Training Learning rule.

III. PROPOSED METHOD

The proposed method is composed of 4 major stages as shown in figure 1. The brain extraction is a necessary step before segmentation. The pixels lying outside the brain contour and which are not of interest share intensity with the structures of interest. By limiting the segmentation to brain, the computation time is reduced. This extraction is done with the help of mathematical morphological operator in stage1, as shown in figure 2(b). and 2D Gaussian filter is applied to the skull stripped image to smoothen it. The smoothened image is shown in figure 2(c).

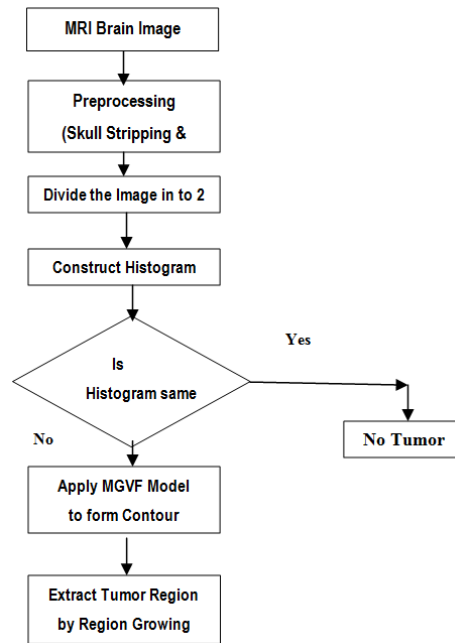


Figure. 1. Proposed Method

In Stage2, the smoothened image is partitioned into 2 halves and the histograms of both the images are subtracted to get the threshold values. If the threshold values are same then the difference will be zero. so, it can be assumed that the image is normal image else, it is proceeded to stage 3. In stage 3, an external force field is created around the abnormal image using MGVF field model. The force vectors from 8-neighbourhood for each pixel is valued. The pixel having the highest score is considered as seed pixel. Using the seed pixel, a region is grown using region growing algorithm and later, in stage4, the area of tumour is calculated.

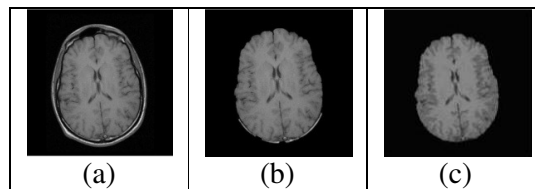


Figure. 2. (a) Input Image (b) Skull Stripped Image (c) Smoothened Image

A. Histogram Thresholding

Histogram is one of the most uncomplicated image segmentation process since thresholding is fast and economical in computation and they require only one pass through the pixels. The histogram of an image represents the relative frequency of occurrence of the various gray levels in the image. This is useful in setting a threshold value to detect the abnormal region.

In our proposed method, after smoothening the skull stripped brain image, it is divided into 2 equal halves along its central axis assuming the brain image is symmetric. The histogram is plotted between the number of pixels and pixel intensity for both the halves. Finally the difference between the two histograms is taken and the resultant difference is plotted. if the image is abnormal then it is proceeded to the next stage. Else, it is assumed the brain is normal and the computation time for segmentation can be minimized.

B. Gradient Vector Flow Model

GVF fields are generated by diffusing the gradient vectors of a gray level or binary edge map, derived from an image [15, 16]. The gradient vector flow field is defined to be vector field. (as in figure 3). $V(x, y) = [u(x, y), v(x, y)]$ (1)

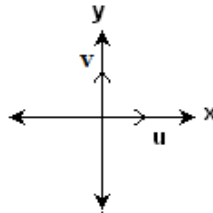


Fig.3. Two-component vector definition for GVF field model

A GVF model as a force field of vectors [15] and they minimized the following energy function to derive the GVF field.

$$E = \iint \mu (|\nabla v|^2 + |\nabla f|^2 |v - \nabla f|^2) dx dy \tag{2}$$

Where, $|\nabla v|^2 = (u^2x + u^2y + v^2x + v^2y)$.

The parameter ‘ μ ’ is a regularization parameter governing the tradeoff between the first and the second term in the integrand. Let a point in ‘n’ dimensional space R^n can be defined by $X = (x^1, x^2, x^3, \dots, x^n)$. The scalar function at X is defined by $f(X) = f(x^1, x^2, x^3, \dots, x^n)$ and the vector function at X is defined by $v(X) = (v^1(x^1, x^2, x^3, \dots, x^n), v^2(x^1, x^2, x^3, \dots, x^n), \dots, v^n(x^1, x^2, x^3, \dots, x^n))$. Assume these functions are defined in a bounded domain $\Omega \subset R^n$ with $\partial\Omega$ as its boundary. GVF is defined as the vector function $v(x)$ in the sobolev space $W_2^2(\Omega)$ [17] that minimize the following function

$$\int_{\Omega} \mu (|\nabla v|^2 + |\nabla f|^2 |v - \nabla f|^2) dx \tag{3}$$

$$\int_{\Omega} \mu \sum_{i=1}^n \sum_{j=1}^n \left(\frac{\partial v^i}{\partial x^j} \right)^2 + \sum_{i=1}^n \left(v^i - \frac{\partial f}{\partial x^i} \right)^2 \sum_{i=1}^n \left(\frac{\partial f}{\partial x^i} \right)^2 dx \tag{4}$$

The above equation (4) can be written in simple

form as, $J = \int_{\Omega} F \left(x^1, \dots, x^n, v^1, \dots, v^n, \frac{\partial v^1}{\partial x^1}, \dots, \frac{\partial v^1}{\partial x^n}, \dots, \frac{\partial v^n}{\partial x^1}, \dots, \frac{\partial v^n}{\partial x^n} \right) dx$

From calculus of variations [18], J is stationary if and only if its first variation vanishes i.e.,

$$\delta J = 0 \tag{5}$$

For every permissible variation $\delta v^i \in W_2^2(\Omega)$, $i=1,2,\dots,n$. By applying the laws of variation[24], 'J' can be derived as,

$$\begin{aligned} \delta J &= \delta \int_{\Omega} F \left(x^1, \dots, x^n, v^1, \dots, v^n, \dots, \frac{\partial v^1}{\partial x^1}, \dots, \right. \\ &\quad \left. \dots, \frac{\partial v^1}{\partial x^n}, \dots, \frac{\partial v^n}{\partial x^1}, \dots, \frac{\partial v^n}{\partial x^n} \right) dx \\ &= \int_{\Omega} \left[\sum_{i=1}^n \frac{\partial F}{\partial v^i} \delta v^i + \sum_{i=1}^n \sum_{j=1}^n \frac{\partial F}{\partial v_j^i} \delta v_j^i \right] dx, \left(v^i \equiv \frac{\partial v^i}{\partial x^j} \right) \\ &= \sum_{i=1}^n \left[\int_{\Omega} \frac{\partial F}{\partial v^i} \delta v^i dx + \int_{\Omega} \sum_{j=1}^n \frac{\partial F}{\partial v_j^i} \delta v_j^i dx \right] \end{aligned}$$

Using integration by parts, we have

$$\delta J = \sum_{i=1}^n \left[\int_{\Omega} \frac{\partial F}{\partial v^i} \delta v^i dx - \sum_{j=1}^n \int_{\Omega} \left(\frac{\partial}{\partial x^j} \right) \frac{\partial F}{\partial v_j^i} \delta v^j dx + \sum_{j=1}^n \int_{\partial \Omega} \frac{\partial F}{\partial v_j^i} \delta v^i \eta^j dS \right]$$

where, η^i is the projection of outward normal unit vector η along x^i axis at $\partial \Omega$ and dS represents the element of area on the boundary $\partial \Omega$. After rearranging the above equation, we get,

$$\delta J = \sum_{i=1}^n \int_{\Omega} \left[\frac{\partial F}{\partial v^i} - \sum_{j=1}^n \frac{\partial}{\partial x^j} \left(\frac{\partial F}{\partial v_j^i} \right) \right] \delta v^i dx + \sum_{i=1}^n \sum_{j=1}^n \int_{\partial \Omega} \frac{\partial F}{\partial v_j^i} \eta^j \delta v^i dS = 0$$

Since variations of v^i , $i=1,2,3,\dots,n$ are independent of each other, it follows that all the coefficients of δv^i in the integrals must each vanish identically in Ω , giving n scalar Euler equation.

$$\frac{\partial F}{\partial v^i} - \sum_{j=1}^n \frac{\partial}{\partial x^j} \left(\frac{\partial F}{\partial v_j^i} \right) = 0 \quad (6)$$

and n boundary conditions

$$\sum_{j=1}^n \left(\frac{\partial F}{\partial v_j^i} \right) \eta^j = 0 \quad (7)$$

Where, $i=1, 2, \dots, n$. Substituting the definition of F in equation (5) and after some algebra, we obtain the Euler equations and boundary conditions for GVF as follows.

$$\mu \sum_{j=1}^n \frac{\partial^2 v^i}{\partial (x^j)^2} - \left(v^i - \frac{\partial f}{\partial x^j} \right) \left(\frac{\partial f}{\partial x^j} \right)^2 = 0 \quad (8)$$

$$\sum_{j=1}^n \frac{\partial v^i}{\partial x^j} \eta^j = 0 \text{ on } \partial \Omega \quad (9)$$

where $i=1,2, \dots, n$. equations (8) and (9) can be written in a simple form using a vector notation as,

$$\mu \nabla^2 v - (v - \nabla f) |\nabla f|^2 = 0 \quad (10)$$

The above equation (10) can be written as

$$\mu \nabla^2 u - (u - f_x) (f_x^2 + f_y^2) = 0 \quad (11)$$

$$\mu \nabla^2 v - (v - f_y) (f_x^2 + f_y^2) = 0 \quad (12)$$

where ∇^2 is the laplacian operator. In homogenous region, $I(x, y)$ is a constant], the second term in each equation is zero because the gradient of $f(x, y)$ is zero. Therefore within such region, 'u' and 'v' are determined by the laplacian equation. Equations 11 and 12 can be solved by treating 'u' and 'v' as function of time stated by Chenyang Xu and J.L Prince, [15] as,

$$u_t(x,y,t) = \mu \nabla^2 u(x,y,t) - [u(x,y,t) - f_x(x, y)]. [f_x(x, y)^2 + f_y(x,y)^2] \quad (13)$$

$$v_t(x,y,t) = \mu \nabla^2 v(x,y,t) - [v(x,y,t) - f_y(x, y)]. [f_x(x, y)^2 + f_y(x,y)^2] \quad (14)$$

The equations 14 and 15 can be rewritten as ,

$$u_t(x,y,t) = \mu \nabla^2 u(x,y,t) - b(x,y)u(x,y,t) + c1(x,y) \quad (15)$$

$$v_t(x,y,t) = \mu \nabla^2 v(x,y,t) - b(x,y)v(x,y,t) + c^2(x,y) \quad (16)$$

Where, $b(x,y) = f_x(x,y)^2 + f_y(x,y)^2$

$c1(x,y) = b(x,y) f_x(x,y)$, $c^2(x,y) = b(x,y) f_y(x,y)$.

To step up the iterative solution, let the indices be i, j and 'n' correspond to x, y and 't' respectively. Spacing between pixels can be Δx and Δy and the time step for each iteration be Δt . Then the required partial derivatives can be approximated as, $u_t = 1/\Delta t (u_{i,j}^{n+1} - u_{i,j}^n)$

$$v_t = 1/\Delta t (v_{i,j}^{n+1} - v_{i,j}^n)$$

Substituting these approximations in to equations (15) and (16) gives the iterative solution to GVF. The value of u and v for each pixel is substituted in to equation (2) to get the energy value E in each iteration. Models based on GVF field can approach object boundaries even if the initial contour is located far from them. However these models still require human interaction. We modify the existing external force field for use in an automatic seed selection and region growing process.

C. Modified GVF Field Model

A Four component field $[k(x,y), l(x,y), m(x',y'), n(x',y')]$ is defined first where k, l, m, n represents the amplitudes (i.e., projections) in the x, y, x', y' axes (as shown in figure 5)

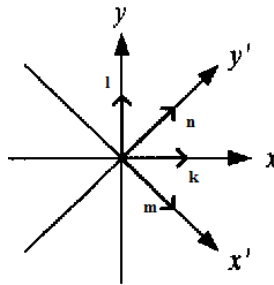


Fig. 4. Four-component vector definition for EGVF field model

Here (x, y) and (x', y') form 2 separate Orthogonal co-ordinate Systems with a rotation of 45° . By Extending the GVF field, the force field can be given as

$$V(x, y) = [V1(x,y), (V2(x, y))]' = [[k,l], [m, n]]' \quad (17)$$

$$V1(x, y) = [k(x, y), l(x, y)]$$

$$V2(x, y) = [m(x, y), n(x, y)]$$

The equation 16 minimizes the energy function as,

$$E = \iint \mu (|\nabla V1|^2 + |\nabla l|^2) + \iint \mu (|\nabla V2|^2 + |\nabla n|^2) + \iint \mu (|\nabla g|^2) - \nabla g \cdot \nabla V \quad (18)$$

Where, $\nabla f = (I_x, I_y)$, $\nabla g = (I_x', I_y')$ are the gradients of Image I in (x, y) and (x', y') co-ordinate Systems. The force vector field $V(x, y)$ can be solved from the following Euler equations by applying calculus of variations to the energy function.

$$\mu \nabla^2 k - (k - I_x) |\nabla f|^2 = 0 \quad (19)$$

$$\mu \nabla^2 l - (l - I_y) |\nabla f|^2 = 0 \quad (20)$$

$$\mu \nabla^2 m - (m - I_x') |\nabla g|^2 = 0 \quad (21)$$

$$\mu \nabla^2 n - (n - I_y') |\nabla g|^2 = 0 \quad (22)$$

where, ∇^2 represents the Laplacian Operator. We can iteratively solve these equations by considering the force vectors (k, l, m, n)'s as function of time n. The time step is simply set to Therefore we get the following iterative equations.

$$k_{n+1} = k_n + \mu \nabla^2 k_n - (k_n - I_x) |\nabla f|^2 \quad (23)$$

$$l_{n+1} = l_n + \mu \nabla^2 l_n - (l_n - I_y) |\nabla f|^2 \quad (24)$$

$$m_{n+1} = m_n + \mu \nabla^2 m_n - (m_n - I_x') |\nabla f|^2 \quad (25)$$

$$n_{n+1} = n_n + \mu \nabla^2 n_n - (n_n - I_y') |\nabla f|^2 \quad (26)$$

The initial conditions are set to $k_0 = I_x$, $l_0 = I_y$, $m_0 = I_x'$, $n_0 = I_y'$ The values of k, l, m and n for each pixel (x, y) are substituted in to Equation (17) to get energy value 'E' in each iteration.

D. Seed selection Process

To search the seeds, we score the status of force vectors from 8-neighborhoods for each pixel. Basically, the score counts the number of neighboring pixels whose force vectors do not point inwards to the considered pixel. All pixels have seed selection scores ranging from 0 to 8. Since the force direction generally indicates the gradient directions onwards object boundary, pixels of higher scores will be chosen as the seeds.

E. Region Growing Process

The region growing approach is as follows,

- 1) Calculate the gray level difference between the seed pixel and the average of pixels surrounding the seed pixel. Let it be ∇ .
- 2) Region is grown from the seed pixel by adding in neighbouring pixels whose value lies within the ∇ value, increasing the size of the region.
- 3) When the growth of one region stops, we simply choose another seed pixel that does not belong to any other region and start again.
- 4) This whole process is continued until all pixels belong to same region.

IV. EXPERIMENTAL RESULTS

we have presented a technique for segmentation and detection of pathological tissues (tumor) from magnetic resonance (MR) images of brain with the help of Histogram, modified gradient vector flow field model and region growing. The proposed technique is designed for supporting the tumor detection in brain images with tumor and without tumor. The obtained experimental results shows that MGVF model can also be used in MRI brain image segmentation.

The proposed method is implemented in normal brain image and the corresponding skull stripped image is shown in figure 5(b) and 5(d). When we compare the histogram plotted for both the sides, they are not symmetrical. The histogram of the right side brain has more intensity when compared to left hand side. This indicates that there may be a tumour on the right hand side of the brain.

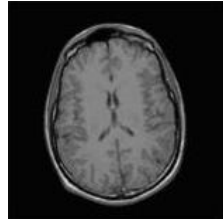


Fig 5(a) Input Image

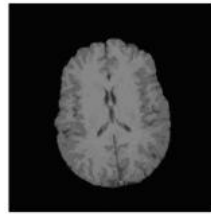


Fig 5(b) Skull stripped

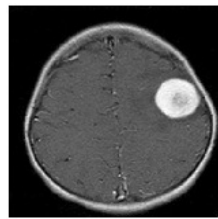


Fig 5(c) Input Image

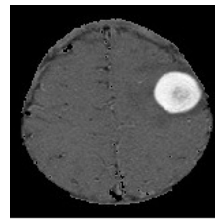
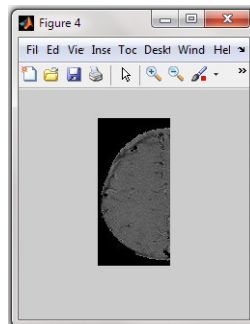
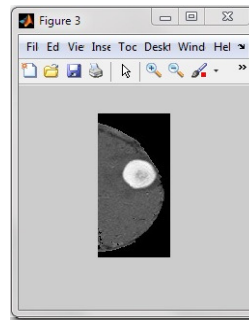


Fig 5(d) Skull stripped

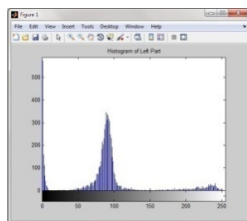


(a)

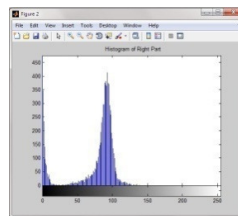


(b)

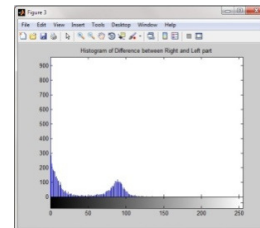
Fig. 6. Partitioned image of Skull stripped brain image, (a) Left Part (b) Right Part



(a)



(b)



(c)

Fig 7. Histogram of (a) left side of the brain, (b) Right side of brain (c) Difference between 2 histogram

Since the two histograms are not same, it can be assumed that the image is abnormal. so, MGVF model is applied to skull stripped image to form the contour near the abnormal region. The image is diffused till the energy curve is saturated as shown in figure 8.

After several iterations, the grey level of the pixels is diffused for scoring to find the seeds. In the figure 9, we can see the arrows are facing outwards i.e., the force vector field is outwards. so, the force moves from the centre of the abnormal region towards the boundary. The image after region growing is shown in figure 10 (a). finally the tumour segmented image is shown in figure 10 (b).

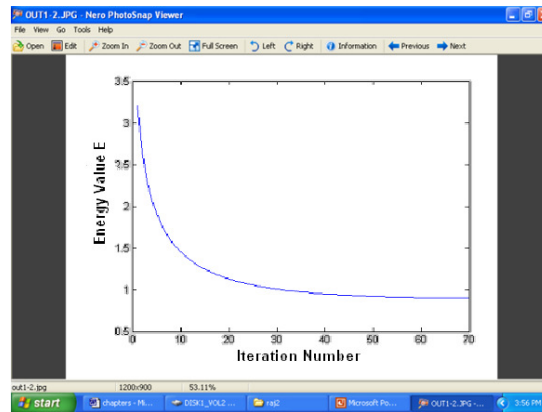


Fig 8. Energy Value Curve

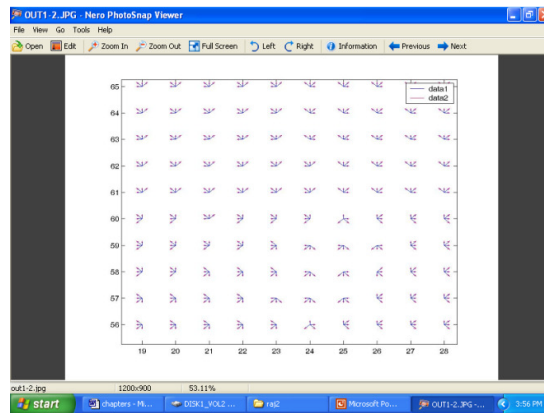


Fig. 9. External force field from seed pixel

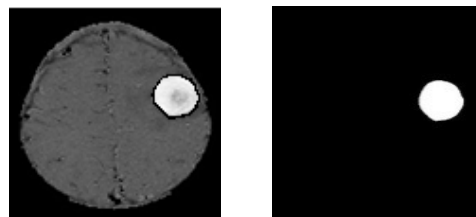
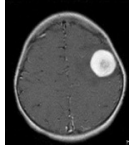
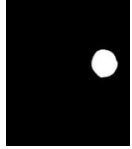
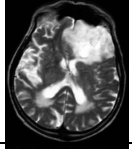
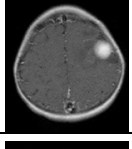
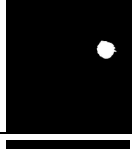
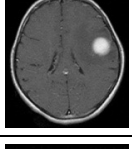
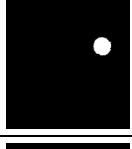
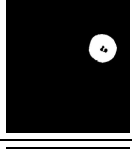
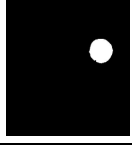
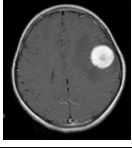
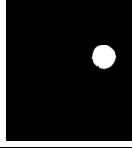


Fig 10 (a) Image after region growing (b) Image after extracting tumour region

Table 1 Experimental Output

<i>Input Image</i>	<i>Image No</i>	<i>Tumour</i>	<i>Area of Tumor (Sq. inch)</i>
	AN1		0.009987
	AN2		0.011092
	AN3		0.00968
	AN4		0.00988
	AN5		0.01042
	AN6		0.00997
	AN7		0.009995

The area of an image is the total number of pixels present in the area which can be calculated in the length units by multiplying the number of pixels with the dimension of one pixel. In our proposed method, the size of the input image is 192x4=198. Therefore, the horizontal resolution is 1/192 inch and the vertical resolution is 1/198 inch. The area of single pixel is equal to (1/192)*(1/198) square inch.

$$\begin{aligned}
 A &= (1/192) * (1/198) \\
 \text{Area of the tumor} &= A * \text{total number of pixels} \\
 &= 2.63 \times 10^{-5} * 380 \\
 &= 0.00999 \text{ sq. inch}
 \end{aligned}$$

PERFORMANCE MEASURE:

The proposed algorithm is applied to MRI brain tumor images and the performance of the algorithm is evaluated using the following measures.

Similarity Index (SI):

$$SI = \frac{2(Ref \cap Seg)}{Ref + Seg} \quad (27)$$

Over Estimated Percentage (OEP):

$$OEP = \frac{(Ref \cap Seg)}{Ref} \times 100 \quad (28)$$

Under Estimated Percentage (UEP):

$$UEP = \frac{(Ref \cap \bar{Seg})}{Ref} \times 100 \quad (29)$$

Correctly Estimated Percentage (CEP):

$$CEP = \frac{(Ref \cap Seg)}{Ref} \times 100 \quad (30)$$

In equations (27) to (30) Ref denotes the volume of the reference and Seg denotes the volume of the segmented image.

The Experimental Output is tabulated in table 1 and the performance measure for segmented image is listed in table 2.

Table 2 Performance Measure

Performance \ Input Image	SI	OEP	UEP	CEP
AN1	93.2	6.6	10.8	97.6
AN2	90.7	5.5	4.6	96.3
AN3	94.9	4.7	5.4	98.8
AN4	96.0	7.3	4.6	94.6
AN5	93.2	6.3	8.8	96.3
AN6	95.7	6.2	2.8	91.4
AN7	96.1	4.1	3.2	94.3

REFERENCES

[1] Selvaraj.,D., Dhanasekaran,R., 2010 “ Novel approach for segmentation of brain magnetic resonance imaging using intensity based thresholding”, 2010 IEEE international conference on communication control and computing technologies, pp 502-507.
 [2] Selvaraj.,D., Dhanasekaran,R., 2010 “ Segmenting internal brain nuclei in MRI brain image using morphological operators”, 2010 International conference on computational intelligence and software engineering, pp 1-4.

- [3] Amit Shrivastava, Monika Shinde, S.S. Gornale and Pratap Lawande, 2007, "An Approach-Effect of an Exponential Distribution on different medical images," International Journal of Computer Science and Network Security, Vol.7, No.9.
- [4] Z. Cho, J. Jones, M. Singh, 1993 "Foundations of Medical Imaging", (New York, NY: John Wiley & Sons,).
- [5] Mohammad Mehdi Khalighi, Hamid Soltanian Zadeh, Caro Lucas, 2002, "Unsupervised MRI segmentation with spatial connectivity", proceedings of SPIE International symposium on Medical Imaging, San Diego, CA, 23-28.
- [6] Jagath C. Rajapakse, Jay N. Giedd, and Judith L. Rapoport, 1997, "Statistical Approach to Segmentation of Single-Channel Cerebral MR Images", IEEE transactions on medical imaging, vol. 16, no. 2.
- [7] Kharrat, A.; Benamrane, N.; Ben Messaoud, M.; Abid, M.; 2007, "Detection of brain tumor in medical images", Proceedings of the 3rd International Conference on Signals, Circuits and Systems (SCS), Medenine, pp: 1 - 6.
- [8] Belma Dogdas, David W. Shattuck, Richard M. Leahy, 2005, "Segmentation of skull and scalp in 3-D human MRI using mathematical morphology", Human Brain Mapping, Vol: 26, No:4, pp: 273 - 285.
- [9] Inan Güler, Ayşe Demirhan, Rukiye Karakis, 2009, "Interpretation of MR images using self-organizing maps and knowledge-based expert systems", Digital Signal Processing, Vol: 19 , No: 4, pp: 668-677.
- [10] John Chiverton, Kevin Wells, Emma Lewis, Chao Chen, Barbara Podda, Declan Johnson 2007, "Statistical morphological skull stripping of adult and infant MRI data", Computers in Biology and Medicine, Vol: 37 , No:3, pp: 342-357.
- [11] Wen-Feng Kuo, Chi-Yuan Lin, Yung-Nien Sun, 2008, "Brain MR images segmentation using statistical ratio: Mapping between watershed and competitive Hopfield clustering network algorithms", Computer Methods and Programs in Biomedicine, Vol: 91, No: 3, pp: 191-198.
- [12] R. Mishra, 2010, "MRI based brain tumor detection using wavelet packet feature and artificial neural networks", Proceedings of the International Conference and Workshop on Emerging Trends in Technology.
- [13] Yan Li and Zheru Chi, 2005, "MR Brain Image Segmentation Based on Self-Organizing Map Network", International Journal of Information Technology, vol. 11, No. 8,.
- [14] D.L. Collins, A.P. Zijdenbos, .Kollokian, C .J. Holmes and A.C. Evans, 1998, "Design and construction of a realistic digital brain phantom" in IEEE Transactions on Medical Imaging, Vol., 17, No.3, PP.463-468.
- [15] Chenyang Xu and J.L Prince, 1998, 'Snakes, shapes and gradient vector flow', IEEE Transactions on image processing, Volume 7, No.3, page 359.
- [16] Chenyang Xu and J.L Prince, 2002, 'Generalized gradient vector flow external forces for active contours', ECCV 2002, LNVS 2352, page 517
- [17] K.E Gustafson, partial differential equations, Newyork, John wiley & sons, 2nd edition.
- [18] R. Courant and D. Hilbert, Method of mathematical physics, Volume 1, Newyork, Interscience.
- [19] R.C. Gonzalez and R.E Woods, 2010, Digital image processing, Pearson Education.
- [20] Bhavna Sharma and Prof K. Venugopalan, "Performance Comparison Of Standard Segmentation Methods For Identification Of Hematoma In Brain CT Scan Images", International journal of Computer Engineering & Technology (IJECET), Volume 3, Issue 1, 2012, pp. 126 - 134, Published by IAEME.
- [21] J. Mohan, V. Krishnaveni and Yanhui Guo, "Performance Analysis Of Neutrosophic Set Approach Of Median Filtering For Mri Denoising", International journal of Electronics and Communication Engineering & Technology (IJECET), Volume 3, Issue 2, 2012, pp. 148 - 163, Published by IAEME.

AUTHOR



D.Selvaraj is an Associate professor in the Department of ECE in Panimalar Engg. college. His specialization in master degree was Medical Electronics from Anna University. Currently he is pursuing his doctoral degree in Sathyabama University, India. He has published 13 papers at various IEEE/ IETE conference and journals.



Dr.R.Dhanasekaran is currently the Director, Research, Syed Ammal Engineering College, Ramanathapuram, India. He obtained his master degree in Power Electronics from Anna University, India. He was awarded Ph.D in Power Electronics from Anna University, India. He has vast teaching experience of 11 years and 3 years in research. He has published more than 40 research papers in various refereed journals and IEEE/ACM conference proceedings. His research interests includes Image Processing, EMI noise in SMPS, Power Electronic circuits.